

Scientific Contributions Oil & Gas, Vol. 48. No. 3, October: 67 - 79

SCIENTIFIC CONTRIBUTIONS OIL AND GAS

Testing Center for Oil and Gas LEMIGAS

Journal Homepage:http://www.journal.lemigas.esdm.go.id ISSN: 2089-3361, e-ISSN: 2541-0520



Real Data-Driven Seismic Low Frequency Extrapolation: A Case Study from The Asri Basin, Java Sea, Indonesia

Ignatius Sonny Winardhi¹, Asido Saputra Sigalingging², and Ekkal Dinanto¹

¹Geophysical Engineering, Institut Teknologi Bandung Ganesha Street No. 10 Bandung, Indonesia.

²Geophysical Engineering, Institut Teknologi Sumatera Terusan Ryacudu Street, South Lampung, Indonesia.

Corresponding author: swinardhi@itb.ac.id.

Manuscript received: June 18th, 2025; Revised: July 11th, 2025 Approved: July 15th, 2025; Available online: October 09th, 2025; Published: October 09th, 2025.

ABSTRACT - The Asri Basin, located in the Java Sea, Indonesia, is a significant hydrocarbon province with regions that remain underexplored. The available legacy seismic data, however, are limited in quality, particularly due to their narrow frequency bandwidth and the absence of low-frequency components. This limitation poses a significant challenge for advanced seismic imaging techniques such as Full Waveform Inversion (FWI), which rely low-frequency data to generate accurate and reliable subsurface models. This study aims to reconstruct the missing low-frequency (<10 Hz) components from the band-limited seismic data to enhance the applicability of FWI. A real-data-driven, self-supervised learning approach for lowfrequency extrapolation is implemented to address this challenge. Using a modified U-Net architecture, the framework is trained directly on the available band-limited seismic data, eliminating the need for synthetic or labeled datasets. The self-supervised workflow employs a frequency-specific masking strategy that enables the model to learn and predict the missing low-frequency content from higher-frequency inputs. The results demonstrate that the proposed method effectively recovers low-frequency signals, achieving accurate reconstruction down to <5 Hz, reducing residual amplitudes compared to conventional methods, and preserving the mid-to-high frequency spectrum. This approach provides a promising solution for overcoming data limitations and mitigating cycle-skipping issues in FWI applications within the Asri Basin and comparable geological settings.

Keywords: low-frequency extrapolation, self-supervised learning, Asri Basin, full waveform inversion.

© SCOG - 2025

How to cite this article:

Ignatius Sonny Winardhi, Asido Saputra Sigalingging, and Ekkal Dinanto, 2025, Real Data-Driven Seismic Low Frequency Extrapolation: A Case Study from The Asri Basin, Java Sea, Indonesia, Scientific Contributions Oil and Gas, 48 (3) pp. 67-79. DOI org/10.29017/scog.v48i3.1748.

INTRODUCTION

Seismic imaging serves as a fundamental technique in subsurface exploration and reservoir characterization, with Full Waveform Inversion (FWI) playing a crucial role in accurately estimating subsurface properties (Virieux & Operto 2009; Tarantola 1986). Low-frequency seismic data are particularly important in mitigating cycle skipping and enhancing the convergence of nonlinear inversion algorithms (Bunks et al., 1995). However, acquiring low-frequency signals is often constrained by the physical limitations of seismic sources and receivers, particularly in geologically complex environments. The absence of these low-frequency components can lead to non-uniqueness in the inversion process and reduce the resolution of the reconstructed subsurface models.

Traditional approaches to addressing the missing low-frequency problem include spectral broadening techniques and model-based extrapolation methods (Claerbout 1992). While these methods have achieved varying levels of success, they often rely on strong assumptions about the data or require significant computational resources, limiting their applicability in large-scale surveys. Frequencydomain analyses, such as spectral decomposition using STFT and CWT, have also been applied in reservoir characterization, highlighting both their potential and limitations (Haris et al., 2019; Diria et al., 2021). In parallel, inversion strategies in alternative domains, such as ray parameter inversion, have been proposed to improve seismic imaging and impedance estimation (Triyoso et al., 2024).

Recent advances in machine learning, particularly deep learning, offer promising alternatives for data reconstruction and enhancement (Yu & Ma 2021). In recent years, convolutional neural networks (CNNs) have demonstrated remarkable performance in various imaging tasks, ranging from image denoising to super-resolution (Jiantao et al., 2021; Sun et al., 2022). Applying deep learning to seismic processing therefore holds significant potential, particularly for low-frequency extrapolation. For example, Sun and Demanet (2018, 2020) employed CNNs to reconstruct low-frequency components directly from band-limited data using a supervised, trace-bytrace strategy in the time domain. Other researchers have refined these methodologies to enhance lowfrequency extrapolation performance (Sigalingging et al., 2021; Sigalingging et al., 2024; Winardhi et al., 2024). Despite promising results on synthetic

datasets, extending these approaches to field data remains challenging due to complexities inherent in real-world signals.

Various strategies have been proposed to improve robustness in field applications. Notably, Fabien-Ouellet (2020) has demonstrated promising results in seismic low-frequency prediction and denoising across both synthetic and real datasets. Similarly, Araya-Polo et al. (2018) have advanced data-driven techniques for low-frequency reconstruction, underscoring the evolving nature of this research field. Collectively, these contributions highlight the importance of developing robust deep learning frameworks capable of generalizing from synthetic models to the complexities of real seismic data.

Among such frameworks, the U-Net, originally developed for biomedical image segmentation (Ronneberger et al., 2015), has proven highly effective in tasks requiring precise localization and contextual understanding. Its encoder-decoder structure, combined with skip connections, enables efficient feature extraction and reconstruction even when training data are limited. In seismic imaging, U-Net-based approaches have recently been explored for noise attenuation and interpolation (Fang et al., 2020). However, most of these methods rely on supervised learning, which requires large labelled datasets that are often unavailable or costly to generate in the seismic domain.

To address these challenges, Cheng et al. (2024) proposed a self-supervised learning methodology that eliminates the need for data, enabling neural networks to be trained directly on real seismic dataset. This paradigm effectively bridges the generalization gap often encountered in supervised learning techniques, which are typically trained on synthetic data.

In this study, self-supervised learning methods are applied to a 2D marine seismic line from the Asri Basin, Java Sea, Indonesia. The Asri Basin is a key hydrocarbon province, with reservoirs primarily originating from syn-rift deposits (Ralanarko et al., 2021). The geological evolution of this basin has been shaped by three major tectonic phases: (1) Rift Initiation during the pre- to early Oligocene, (2) Syn-Rift from the early to late Oligocene, and (3) Post-Rift (Sukanto et al. 1998). These tectonic processes have produced complex structural configurations, necessitating advanced seismic imaging techniques such as FWI for accurate subsurface characterization. However, legacy seismic data from the Asri Basin

often suffer from poor quality due to a band-limited frequency spectrum, where low frequencies are missing as a result of acquisition constraints. This deficiency poses significant challenges for seismic imaging, particularly for FWI, which relies on a broad frequency range to achieve high-resolution subsurface models. To overcome this limitations, this study focuses on reconstructing the missing low-frequency components using self-supervised deep learning techniques. The reconstructed lowfrequency data serve as a critical preparatory step for enhanced seismic imaging, ultimately improving the outcomes of reprocessing legacy seismic data from the Asri Basin.

METHODOLOGY

Self-supervised learning

Self-supervised learning (SSL) for low-frequency seismic extrapolation, as proposed by Cheng et al. (2024), utilizes the classical U-Net architecture (Ronneberger et al., 2015). A key advantage of SSL is its ability to generate training pairs (inputs and labels) directly from observed data, eliminating the need for manually labeled datasets. This approach draws inspiration the Noisier2Noise method in the machine learning community (Moran et al., 2020). In the Noisier2Noise framework, the training process relies solely on the original noisy observations: additional noise is deliberately added to create a noisier dataset, while the original noisy data serve as pseudo-labels. This strategy enables the neural network to learn noise characteristics and reconstruct the desired signal without requiring a clean reference data.

Following this principle, LessLow-to-Low (L2L) framework is introduced for low-frequency prediction. In L2L, seismic data with reduced lowfrequency content are used as input to predict data with relatively richer low-frequency content. The method assumes that available seismic waveform data, although lacking sufficient low-frequency energy due to acquisition constraints, can still act as pseudo-labels. These waveforms typically lack sufficient low-frequency content due to acquisition constraints. To create the input for the network, a high-pass filter to the original data is applied, thereby, further attenuating the already diminished lowfrequency components. In this setup, the high-pass filtered data, referred to as the "less low" dataset, serves as the input, while the original waveforms (with relatively more low-frequency content) act as

the pseudo-labels. Thus, the L2L framework operates as a supervised learning proses in which input-label pairs are derived from the data itself, exemplifying the concept of self-supervised learning. This allows the method to be applied directly to real seismic datasets without requiring external labels. SSL for low-frequency extrapolation primarily consists of two components: a warm-up phase and iterative data refinement (IDR). The warm-up phase, supervised learning is performed on synthetic datasets generated from simulated subsurface models. Inputs are created by applying a high-pass filter to the synthetic data, while the unfiltered data serve as targets. This 'less-to-low" dataset is used to pretrain the model for a set number of epochs, producing an initial backbone model. In the IDR phase, the pretrain model is iteratively refined using field seismic data. Predictions from model serve as pseudo-labels while corresponding inputs are generated by applying a high-pass filter to those predictions. In the first iteration, the warm-up model is used to predict the original seismic data. At each iteration, the model is trained for only one epoch, after which the updated model replaces the previous one, ensuring progressive refinement.

Deep learning architecture

The SSL framework introduced by Chen et al. (2024) for low-frequency tasks utilizes a conventional U-Net architecture. In this study, we adapt and modify the U-Net to better address seismic los-frequency extrapolation. The details of the modified architecture are illustrated in Figure 1. The model consists of five scales, with 2×2 downsampling and 2×2 up-sampling operations. Each block contains two consecutive convolutional layer, each with a 3×3 kernel and Leaky Rectified Linear Unit (Leaky ReLu) activation. Batch normalization is not applied. The number of filters in both the encoder and decoder is set to 96, with the final layer reduced to 48 filers. The complete filter distribution is depicted in Figure 1.

To train the network, a hybrid loss function that combines data loss and amplitude spectrum loss was employed. The hybrid loss function is formulated using the Mean Absolute Error (MAE) and can be expressed as:

$$Loss(L, O) = \frac{1}{N} \sum_{i=1}^{N} |L_i - O_i|$$
 (1)

where L represents the label data, and O denotes the output of the models.

Training prosedur

As described earlier, the model is trained in two stages: Warm-Up and Iterative Data Refinement (IDR). The detailed workflow is presented in Figure 2 and described as follows:

Stage 1 preparation of dataset:

In this stage, we generate a synthetic dataset using the Marmoussi2 velocity models (Figure 3). The simulation parameters are provided in Table

1. The first receiver is positioned at 25 m from the left boundary of the model, while the first shot is located at 0 m. Receiver positions remain fixed for all shot locations. The data simulation is conducted using the Julia programming language with the JUDI framework (Witte et al. 2019). After generating the shot data, the data are randomly cropped into patches of 128×128 pixels, resulting in a total of 9,050 image samples.

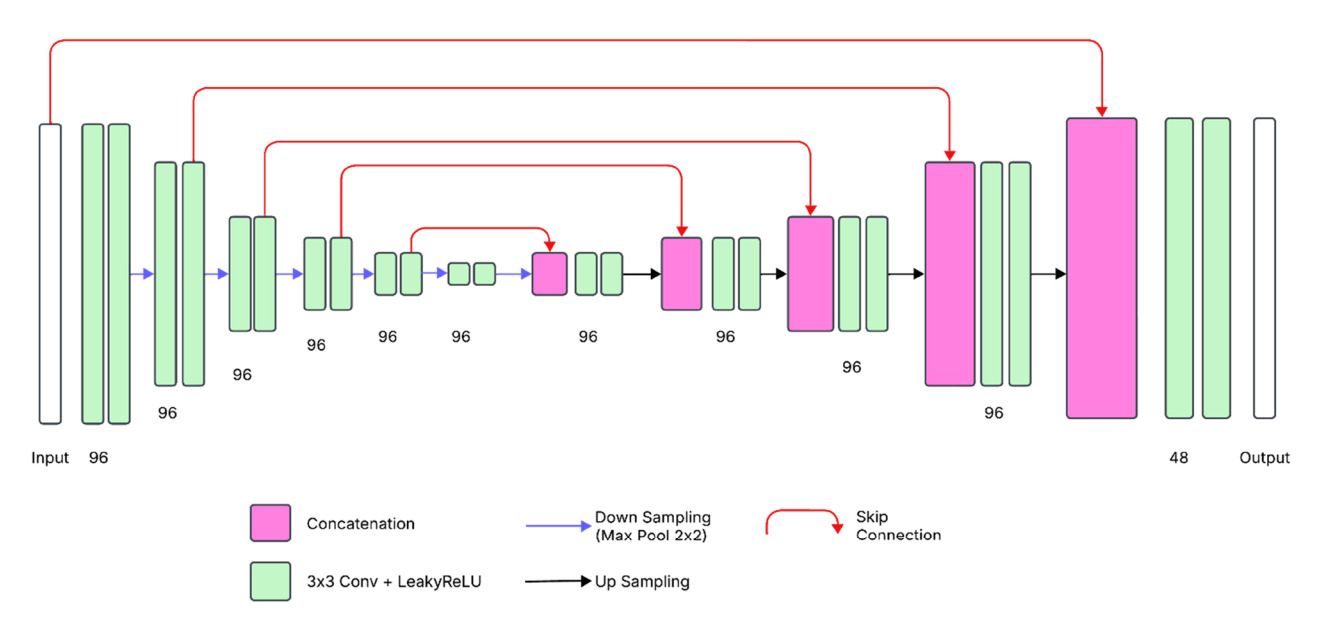


Figure 1. The deep-learning U-Net architecture used in this study.

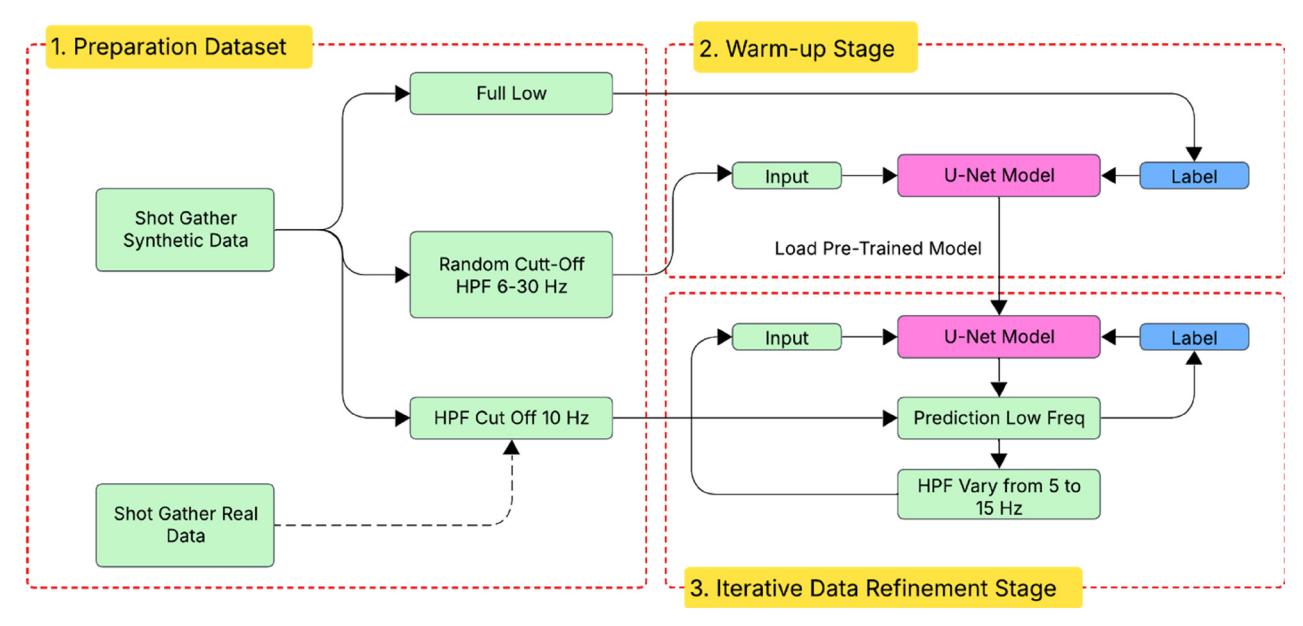


Figure 2. Workflow of self-supervised learning for low-frequency extrapolation.

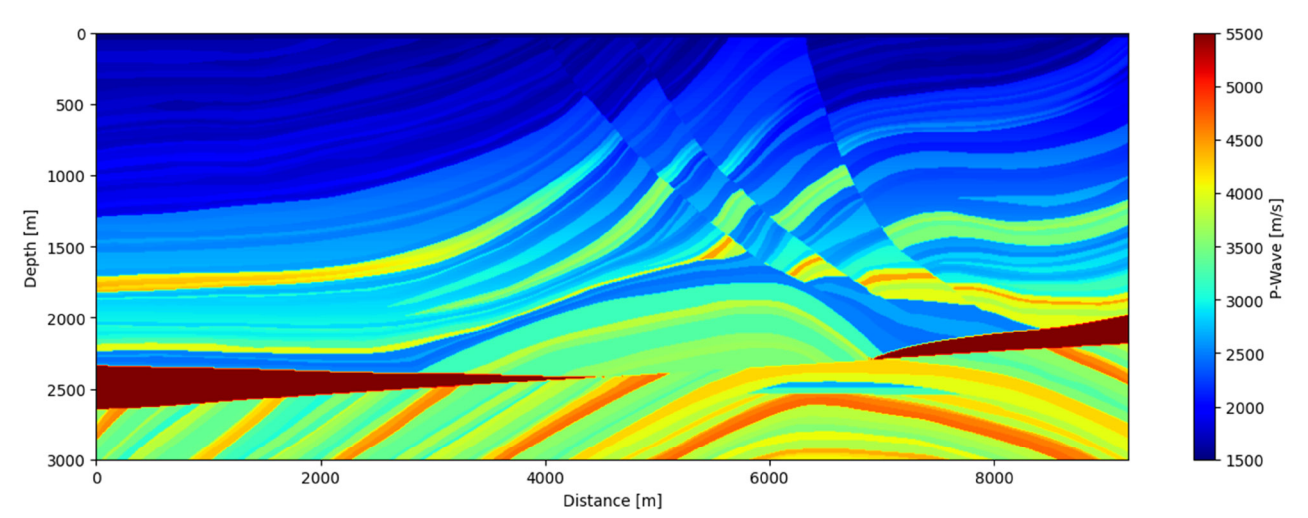


Figure 3. Marmousi2 P-wave velocity model used to generate synthetic shot gathers. The model exhibits strong lateral and vertical velocity variations representing complex geological structures such as faults, anticlines, and stratigraphic layering. These heterogeneities make it a standard benchmark model for testing seismic imaging and inversion algorithms.

Stage 2 warm-up stage:

The image patches from Stage 1 are used for initial training. The label data consist of original image patches, while the input data are generated by applying a high-pass filtering with a randomly selected cutoff frequency between from 5 to 30 Hz, producing band-limited inputs. The model is trained for 150 epochs, using a decaying learning rate (LR) strategy: the initial LR is set to 0.001 and decays by 0.9 every 30 iterations. Optimization is performed with the Adam optimizer and a batch size of 64. The optimal model obtained at the end of this stage is carried forward to stage 3.

Table 1. Simulation parameter to generate synthetic data.

Parameters	Values
Velocity Models	2D Marmoussi2
Grid Spacing	10 x 10 (m)
Grid Number	920 x 300
Number Receiver	361
Number Shot	181
Receiver Spacing	25 (m)
Shot Spacing	50 (m)
Sampling time	0.002(s)
Time length	3 (s)
Wavelet	Ricker
Source Frequency	15 Hz

Stage 3 iterative data refinement (IDR)

At this stage, synthetic data are further used to ensure that the model generalizes across diverse data patterns. The IDR is the cornerstone of selfsupervised learning (SSL) framework, introducing a novel mechanism for generating input-label pairs without requiring ground truth. The pretrained model from Stage 2 is used for prediction in the first iteration. The input data are the same band-limited dataset used in Stage 2. The model outputs are treated as pseudo-labels. A high-pass filter is the applied to these outpurs to generate the corresponding inputs. The model is trained for a single epoch with these new input-label pairs. This process is repeated for 300 iterations. At each iteration, the updated model from the previous step is used, and a new set of input-label pairs is generated. Through this iterative refinement, the model progressively improves its capacity to reconstruct low-frequency content from extrapolation from band-limited dataset. The learning rate at this stage decays by a factor of 0.9 every 50 epochs.

After obtaining a robust backbone model trained on the synthetic dataset, we applied it to our real seismic marine dataset. The raw field data underwent standard pre-processing to minimize noise and enhance data quality. The pre-processing steps included applying a low-pass filter with a cutoff frequency below 10 Hz, a notch filter to remove specific frequency components, and De-Multiple processing to suppress multiple reflections. Following these steps, the data were prepared according to the procedure outlined in Stage 1, and the iterative data refinement (IDR) process was repeated in the same manner as previously implemented.

The implementation of training process was performed on a system equipped with an NVIDIA GeForce RTX 3060 GPU, an Intel Core i7 13th Generation processor, and 64 GB of RAM, and it leveraged the TensorFlow 2.0 Python framework.

RESULT AND DISUCUSSION

Synthetic testing

We validate the workflow of self-supervised learning (SSL) low-frequency extrapolation using synthetic data. Figure 4a shows the original simulated shot gather generated from the Marmoussi2 model, while Figure 4b displays its corresponding frequency spectrum. The model accuracy was evaluated by predicting low-frequency components from input data processed with different high-pass filter cutoff frequencies.

Figure 5 illustrates the results for different highpass filter (HPF) cutoff frequencies, demonstrating various test scenarios for the SSL prediction model with varying degrees of missing low-frequency content in the input data. The corresponding predictions are presented in Figures 5b, 5e, and 5h for HPF cutoffs of 5, 10, and 15 Hz, respectively, while the residuals computed as the difference between the predicted data and the original shot data (Figure 4a) are displayed in Figures 5c, 5f, and 5i for 5, 10, and 15 Hz, respectively. These results indicate that the model accurately predicts the missing low-frequency components when the input data lacks frequencies below 5 Hz and 10 Hz. However, prediction error increases, as reflected in higher residual amplitudes, when a greater protion of the low-frequency band is absent, particularly in the case of the 15 Hz HPF input.

To further verify both waveform reconstruction and spectral band, a single trace was extracted from the test shot data. Figure 6a compares the original waveform with the predicted data derived from inputs with varying degrees of missing low-frequency content. The extrapolated waveform closely matches the original, particularly for input cutoff below 10 Hz. However, when low-frequency information is firther reduced (i.e., cutoff at 10 Hz), discrepancy between the predicted and original waveforms gradually increases; nonetheless, phase alignment remains nearly perfect. Overall, the method reconstructs waveforms that are highly consistent with the original data.

Since the cycle-skipping problem in Full Waveform Inversion (FWI) primarily arises from phase mismatches, the accurate phase reconstruction demonstrated here suggests that cycle skipping can be effectively minimized.

Figures 6b - 6d present the spectral analyses of the original, input, and predicted data for HPF cutoffs of 5 Hz, 10 Hz, and 15 Hz, respectively. As in the waveform analysis, the spectral results confirm that the SSL model successfully reconstructs missing low-frequency content. In these Figures, the blue line represents the original spectrum, the orange line denotes the predicted spectrum, and the green line indicates the input data spectrum. Notably, even when the input data contain severely attenuated

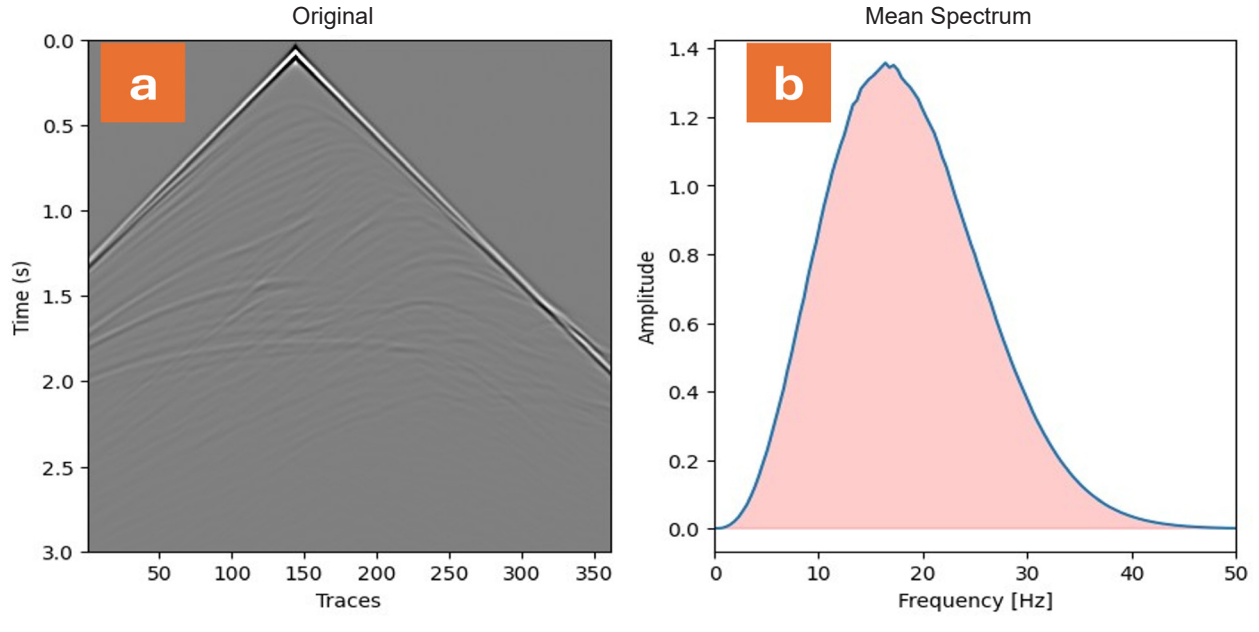


Figure 4. (a) Synthetic shot gather generated from the Marmousi2 P-wave velocity model using a Ricker wavelet source with a dominant frequency of 15 Hz. The reflectivity pattern demonstrates strong amplitude variations caused by complex subsurface structures. (b) Corresponding mean amplitude spectrum of the shot gather shown in (a), illustrating the frequency content centered around the dominant frequency of the source wavelet.

low-frequency components, the model recovers frequencies, even down to levels below 2 Hz. This result underscores the accuracy, stability, and overall reasonability of the proposed SSL low-frequency extrapolation algorithm, demonstrating its robust capability to reconstruct essential low-frequency information from incomplete input data.

Figure 8a, 8d, and 8f show test shot datasets derived from applying high-pass filters with cut-off frequencies of 5 Hz, 10 Hz, and 15 Hz, respectively, to the original seismic data. These filtered datasets

serve as inputs for our self-supervised learning (SSL) model, and the corresponding prediction results are displayed in Figures 8b, 8e, and 8g.

To assess the model accuracy, spectral analysis on a single trace was conducted, as shown in Figure 9. The analysis demonstrates that the SSL model effectively reconstructs energy at frequencies below 5 Hz, even though the input data primarily cover frequencies above 7 Hz; Indicating its capability to predict the spectrum in the missing low-frequency range.

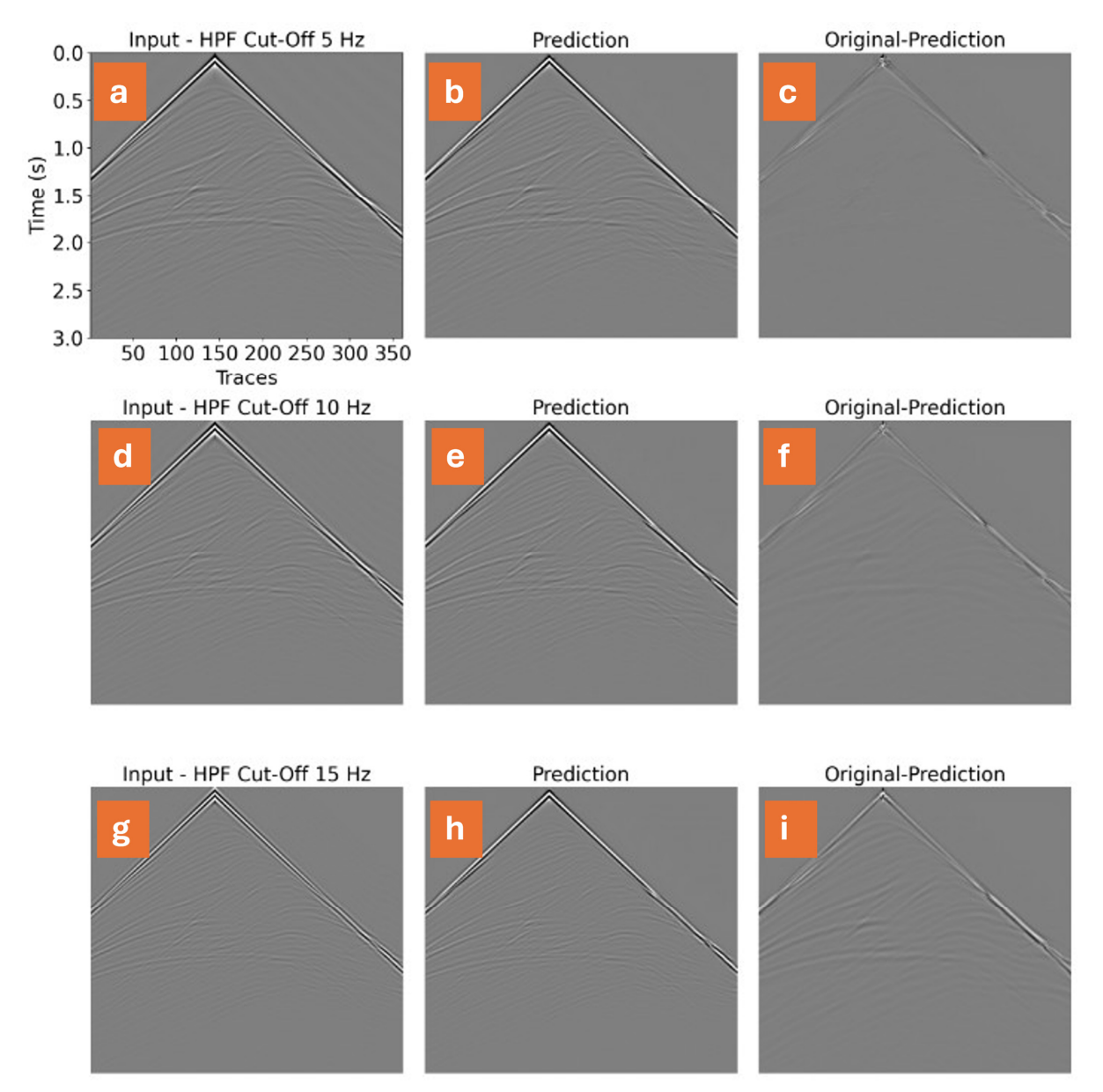


Figure 5. Results of testing low-frequency data. The model's accuracy is evaluated by predicting low-frequency components from input data with different high-pass filter (HPF) cutoff frequencies: (a) 5 Hz, (d) 10 Hz, and (g) 15 Hz. The corresponding predictions obtained using the self-supervised learning (SSL) model are shown in (b) 5 Hz, (e) 10 Hz, and (h) 15 Hz. To assess prediction quality, the residuals—computed as the difference between the predicted data and the original shot data in Figure 4a—are displayed in (c) 5 Hz, (f) 10 Hz, and (i) 15 Hz.

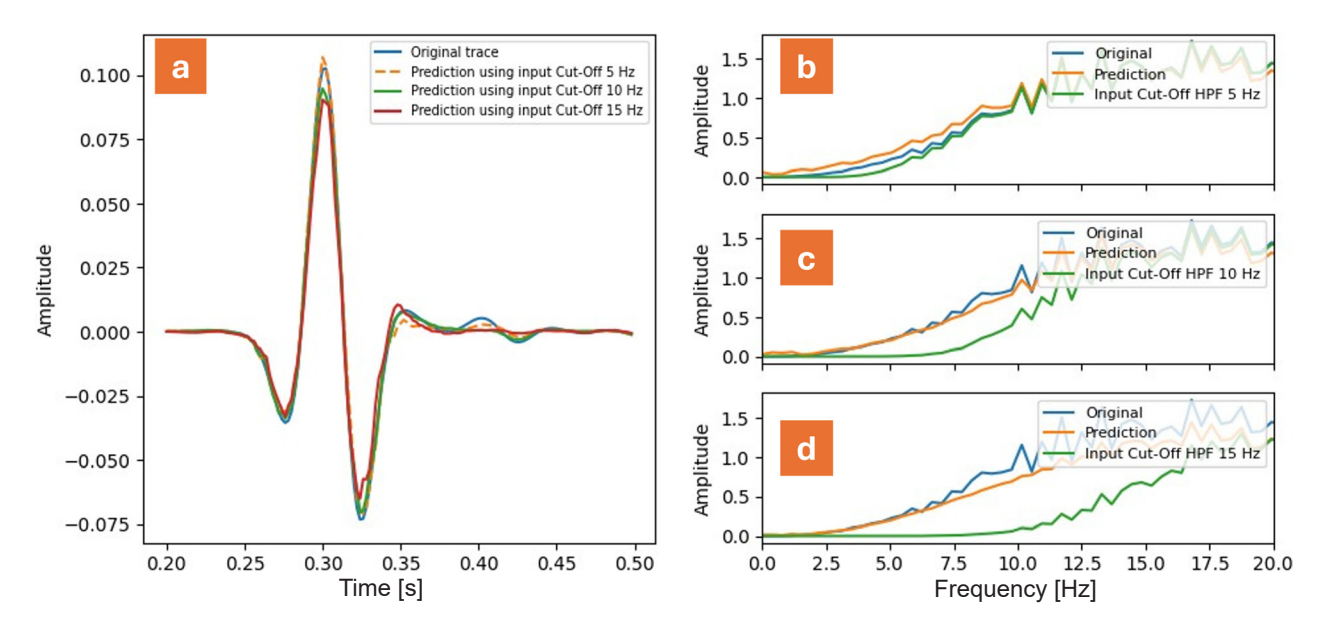


Figure 6. (a) Comparison between the original seismic trace and the predicted traces generated using input data filtered with different high-pass filter (HPF) cutoff frequencies of 5, 10, and 15 Hz. The prediction accuracy decreases with higher cutoff frequencies due to the loss of low-frequency components essential for waveform reconstruction. (b–d) Corresponding amplitude spectra of the predicted traces for each HPF case, illustrating the spectral energy shift and attenuation effects caused by different filtering levels.

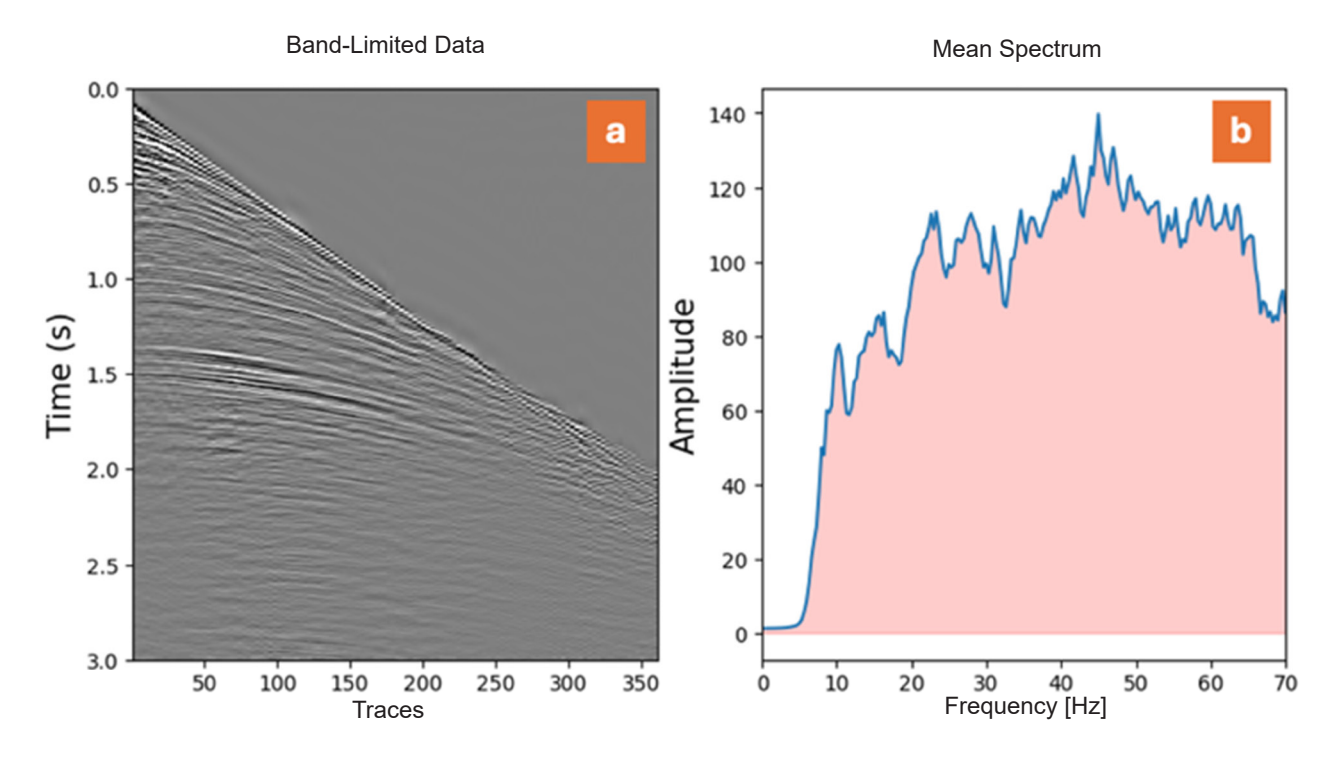


Figure 7. Real marine seismic data from the Asri Basin. (a) Band-limited shot gather used as the input data for low-frequency prediction. (b) Mean amplitude spectrum of the band-limited data, showing a dominant frequency around 35–40 Hz with an effective bandwidth between approximately 10 and 70 Hz, indicating the absence of low-frequency components (<10 Hz) to be reconstructed by the prediction model.

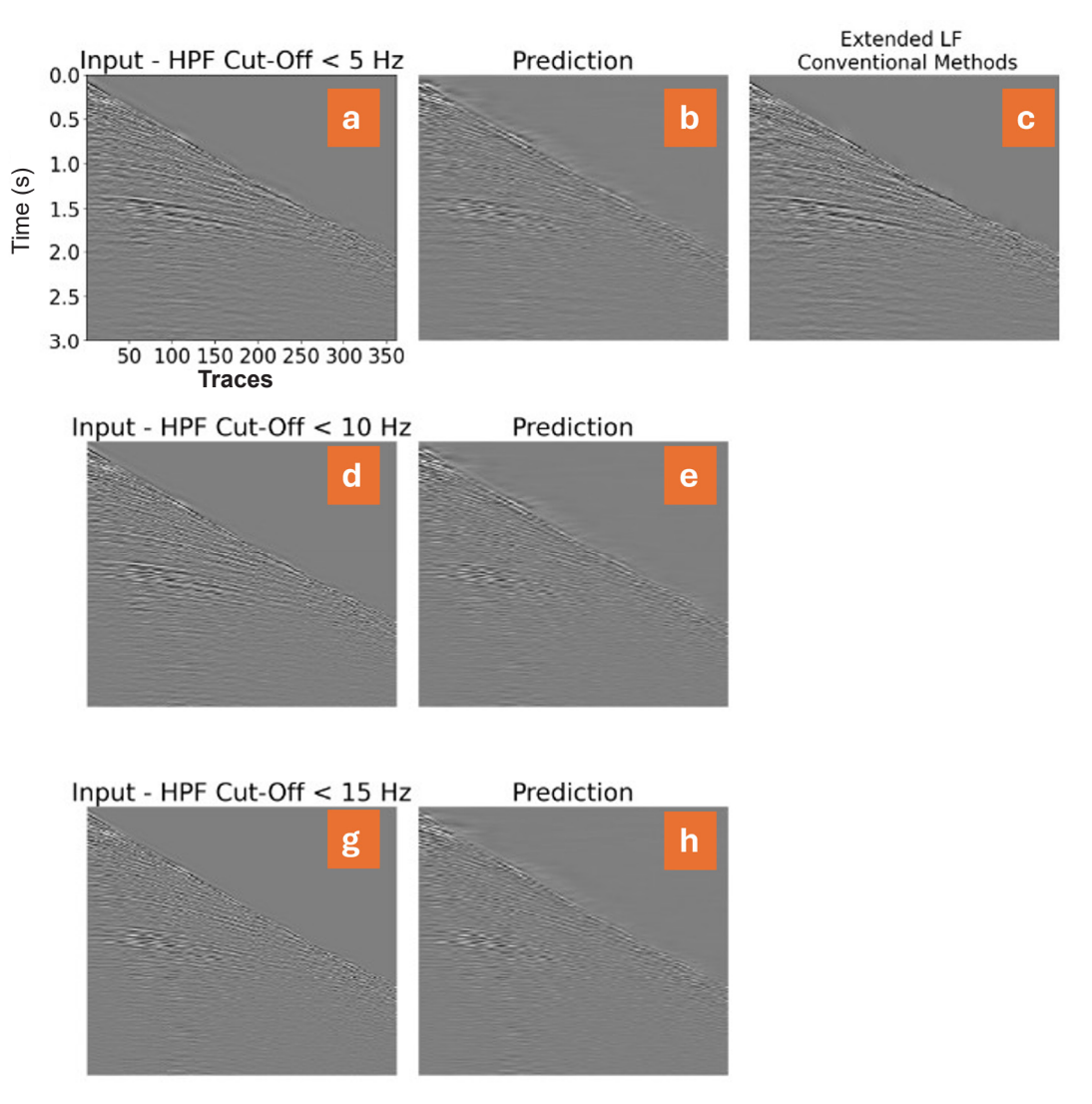


Figure 8. (a), (d), and (f) present test shot datasets obtained by applying high-pass filters with cut-off frequencies of 5 Hz, 10 Hz, and 15 Hz, respectively, to the original seismic data. These filtered datasets serve as inputs to the self-supervised learning (SSL) model, with the corresponding prediction results displayed in Figures 8(b), (e), and (g). In contrast, Figure 8(c) shows the full-band seismic data processed using conventional methods.

Furthermore, the energy spectrum of the data predicted was compared by the SSL model with that obtained using conventional methods, as illustrated in Figures 9a–9c. This comparison reveals a strong correlation between the two spectra, validating the proposed approach. More importantly, the SSL model reconstructs the energy at very low frequencies (below 5 Hz) more accurately, whereas conventional methods tend to lose energy in this range. The results discussed above validate that our SSL model effectively reconstructs the low-frequency components of the Asri Basin dataset. Moreover, spectral analysis reveals that the model not only accurately predicts low-frequency content but also preserves the mid-to-high frequency information. This performance underscores the advantage of the real-data-driven approach: the SSL model extracts comprehensive spectral information directly from real seismic data, maintaining the original spectral range. In contrast, models trained on synthetic data characterized by a narrower spectral range often have narrower spectral bandwidth, often show limited performance in frequency reconstruction.

Despite the promising results, the proposed approach has several limitations that warrant further investigation. First, the self-supervised learning (SSL) model addresses the input-output mapping as a highly non-linear problem, making its performance strongly dependent on the specific dataset used during training. Due to constraints in the current training tools, the available dataset is limited, which restricts the model's ability to generalize effectively

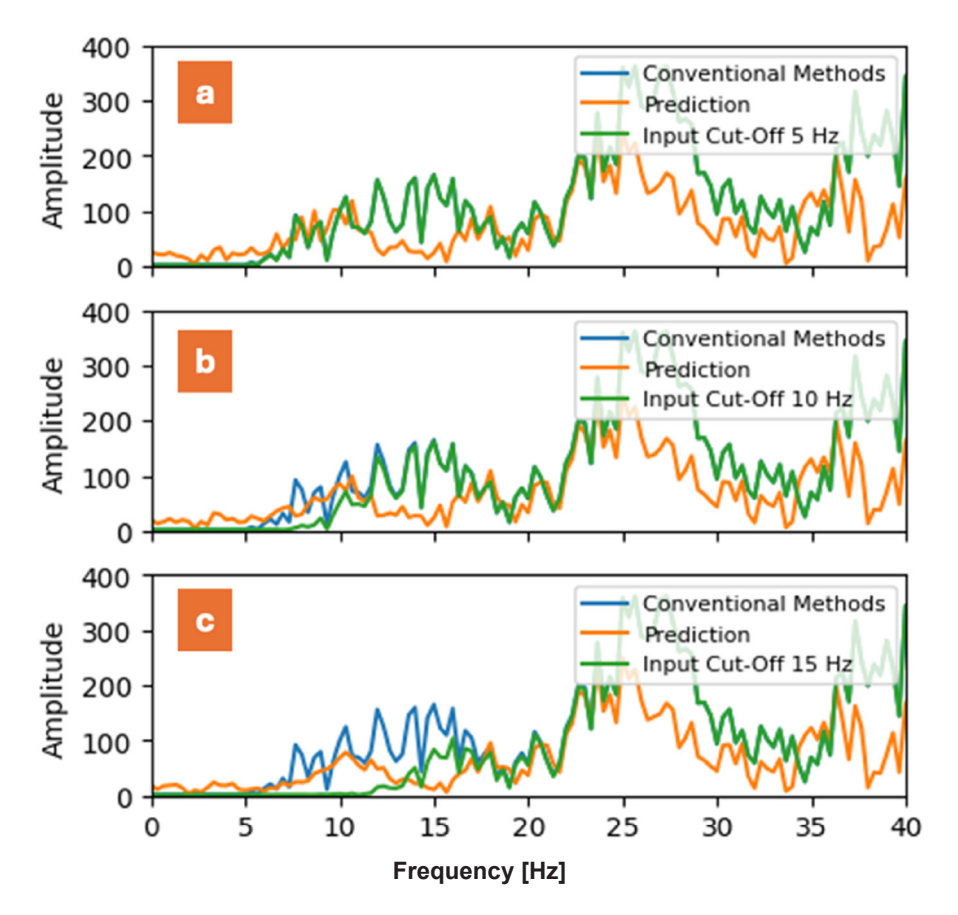


Figure 9. Shows a comparative spectral analysis of field data from the Asri Basin. In each subplot, the spectral response of a single trace is displayed using three lines: the blue line represents data reconstructed by conventional extended frequency methods, the orange line shows the prediction by the SSL model, and the green line denotes the input data processed with a specific low-frequency cut-off. Subplot (a) corresponds to a 5 Hz cut-off, subplot (b) to a 10 Hz cut-off, and subplot (c) to a 15 Hz cut-off.

to other blind datasets. Expanding the training dataset is therefore essential to enhance the robustness and generalizability of the approach. Furthermore, the model's resilience to the cycle-skipping problem; a common challenge in full waveform inversion (FWI) has not yet been fully validated. To thoroughly assess the accuracy and robustness of our SSL model, it is necessary to conduct additional experiments using both synthetic and real seismic data from the Asri Basin. Such evaluations will help determine how well the model can maintain accurate frequency reconstruction, particularly in challenging scenarios where cycle skipping might occur.

Another limitation arises from the inherent noise in real seismic datasets. Although noise-reduction techniques were applied during preprocessing, we have taken measures to minimize noise, residual noise likely remains and may impact the robustness and accuracy of the predictions. This residual noise can introduce variability into the reconstructed energy spectrum, ultimately influencing the overall

performance of the model. Taken together, these limitations introduce a degree of uncertainty into the current predictions. The combined effects of dataset dependency, potential cycle skipping, and residual noise emphasize the need for further validation and refinement. Addressing these challenges will be critical to improving the reliability of the SSL model and ensuring its applicability to a broader range of real-world seismic data processing tasks.

CONCLUSION

In this study, we introduced a self-supervised learning (SSL) model designed to reconstruct the low-frequency components of seismic data, with a specific focus on the Asri Basin dataset. Our approach effectively preserves the full spectral range, as demonstrated by spectral analyses that reveal strong correlations between the energy spectra predicted by the SSL model and those obtained via conventional methods. Notably, the SSL model

Band-limited

accurately reconstructs low-frequency energy (below 5 Hz), addressing a common shortcoming in conventional techniques that typically lose energy in this range.

Despite these promising results, several limitations remain. The performance of the SSL model is highly dependent on the training dataset, which is currently limited due to constraints in available tools and data. This dataset dependency raises concerns about the model's generalizability to other blind datasets. Furthermore, the issue of cycle skipping a well-known challenge in full waveform inversion requires additional validation through experiments on both synthetic and real seismic data. Finally, although preprocessing techniques were applied to reduce noise in the real datasets, residual noise may still affect the robustness and accuracy of the model's predictions. Overall, the findings underscore the potential of SSL as a robust, realdata-driven approach for seismic data reconstruction. Future work should focus on expanding the training dataset, systematically evaluating the model performance against cycle skipping, and mitigating the effects of residual noise. Addressing these challenges will be crucial for enhancing the reliability and applicability of SSL-based methods in diverse seismic exploration scenarios.

ACKNOWLEDGMENT

We would like to express our sincere gratitude to Upstream Research & Technology Innovation PT. Pertamina for providing the necessary resources, data and support that made this research possible. We also extend our gratitude to our colleagues and collaborators for their valuable contributions to data collection and analysis.

GLOSSARY OF TERMS

Symbol	Description	Unit
Adam	Adaptive Moment Estimation optimizer used to accelerate the training process in deep learning.	-
Asri Basin	A hydrocarbon basin located in the Java Sea, Indonesia, and the focus area of this case study.	_

Data	restricted frequency bandwidth due to acquisition limitations.	112
CNN (Convolutional Neural Network)	A deep learning architecture based on convolution operations, widely applied in image and seismic data processing.	_
Epoch	One complete pass of the entire dataset through the training process of a model.	_
FWI(Full	A seismic inversion method	_
Waveform	that uses the full waveform	
Inversion)	to obtain a detailed subsurface model.	
HPF(High-Pass Filter)	A filter that passes high- frequency components while attenuating low- frequency components.	Hz
IDR(Iterative Data Refinement)	A stage in SSL where input–label pairs are regenerated iteratively, and the model is updated in each iteration.	_
L2L (Less-Low-to-Low)	A self-supervised framework for predicting data with enhanced low-frequency content from data with reduced low-frequency content.	_
LearningRate (LR)	A parameter that controls the step size of weight updates during model training.	_
MAE (Mean Absolute Error)	A loss function measuring the average absolute difference between predictions and labels.	_
Marmoussi2 Model	A synthetic seismic velocity model commonly used for testing inversion methods.	m/s
Ricker Wavelet		Hz
SSL(Self- Supervised Learning)	A deep learning paradigm that generates pseudo-labels from the data itself without requiring manually labeled datasets.	_
U-Net	An encoder–decoder deep learning architecture with	_

Seismic data with a

Hz

skip connections, applied in segmentation and seismic reconstruction tasks.

REFERENCES

- Araya-Polo, M., Jennings, J., Adler, A. & Dahlke, T. (2018). Deep-learning tomography, The Leading Edge, 37(1), 58–66, https://doi.org/10.1190/tle37010058.1.
- Bunks, C., Saleck, F. M., Zaleski, S., & Chavent, G. (1995). Multiscale seismic waveform inversion. Geophysics, 60(5), 1457–1473. https://doi.org/10.1190/1.1443880.
- Cheng, S., Wang, Y., Zhang, Q., Harsuko, R., & Alkhalifah, T. (2024). A self-supervised learning framework for seismic low-frequency extrapolation, Journal of Geophysical Research: Machine Learning and Computation, 1, e2024JH000157, https://doi.org/10.1029/2024JH000157.
- Claerbout, J. F. (1992). Earth Sounding Analysis: Processing versus Inversion, Blackwell.
- Diria, S. A., Purba, H., & Tampubolon, R. A. (2017). Identifikasi Reservoir Dan Hidrokarbon Dengan Menggunakan Metode Synchrosqueezing Transform (Reservoir and Hydrocarbon Identification Using Synchrosqueezing Transform). Lembaran publikasi minyak dan gas bumi, 51(3), 179-191. https://doi.org/10.29017/LPMGB.51.3.29.
- Fabien-Ouellet, G. (2020). Low-frequency generation and denoising with recursive convolutional neural networks, in SEG Technical Program Expanded Abstracts 2020, Society of Exploration Geophysicists, pp. 870–874.
- Fang, W., Fu, L., Zhang, M. & Li, Z. (2020). Seismic data interpolation based on U-Net with texture loss, Geophysics, 86, 1–107, https://doi.org/10.1190/geo2019-0615.1.
- Haris, A., & Riyanto, A. (2017). Spectral decomposition technique based on STFT and CWT for identifying the hydrocarbon reservoir. Scientific Contributions Oil and Gas, 40(3), 125-

- 131. https://doi.org/10.29017/SCOG.40.3.125-131
- Li, J., Wu, X. & Hu, Z. 2021, Deep learning for simultaneous seismic image super-resolution and denoising, IEEE Transactions on Geoscience and Remote Sensing, PP, 1–11, https://doi.org/10.1109/TGRS.2021.3057857.
- Moran, N., Schmidt, D., Zhong, Y. & Coady, P. 2020, Noisier2Noise: Learning to denoise from unpaired noisy data, in Proceedings of the IEEE/CVF Conference on Computer Vision and Pattern Recognition (CVPR) 2020, pp. 12061–12069, https://doi.org/10.1109/CVPR42600.2020.01208.
- Ralanarko, D., Wahyuadi, D., Nugroho, P., Rulandoko, W., Syafri, I., Abdurrokhim, A., & Nur, A. (2021). Seismic expression of Paleogene Talangakar Formation Asri & Sunda Basins, Java Sea, Indonesia, Berita Sedimentologi, 46, 21–43, https://doi.org/10.51835/bsed.2020.46.1.58.
- Ronneberger, O., Fischer, P. & Brox, T. (2015). U-Net: Convolutional networks for biomedical image segmentation, in Medical Image Computing and Computer-Assisted Intervention MICCAI 2015: 18th International Conference, Munich, Germany, October 5–9, 2015, Proceedings, Part III, vol. 18, pp. 234–241.
- Sigalingging, A.S., Winardhie, I.S. & Dinanto, E. (2021). Ekstrapolasi frekuensi rendah pada Full Waveform Inversion (FWI) dengan menggunakan deep learning. Part 1: Validasi data sintetik, Jurnal Geofisika, 19(2), 74–79.
- Sigalingging, A.S. et al. (2024). Application of deep learning for low-frequency extrapolation to marine seismic data in the Sadewa Field, Kutei Basin, Indonesia, in Bezzeghoud, M. et al. (eds), Recent Research on Geotechnical Engineering, Remote Sensing, Geophysics and Earthquake Seismology. MedGU 2022. Advances in Science, Technology & Innovation, Springer, Cham, viewed, https://doi.org/10.1007/978-3-031-48715-6 51.
- Sukanto, J., Nunuk, F., Aldrich, J.B., Rinehart, G.P. & Mitchell, J. (1998). Petroleum system of the Asri Basin, Java Sea, Indonesia', in Proceedings of the 26th Annual Convention,

- Indonesian Petroleum Association.
- Sun, H. & Demanet, L. (2018). Low-frequency extrapolation with deep learning, in SEG Technical Program Expanded Abstracts 2018, Society of Exploration Geophysicists, pp. 2011-2015.
- Sun, H. & Demanet, L. (2020). Extrapolated full-waveform inversion with deep learning, Geophysics, 85(3), R275–R288, https://doi. org/10.1190/geo2019-0195.1.
- Sun, Q.F., Xu, J.Y. & Zhang, H.X. (2022). Random noise suppression and super-resolution reconstruction algorithm of seismic profile based on GAN, Journal of Petroleum Exploration and Production Technology, 12, 2107–2119, viewed [date], https://doi.org/10.1007/s13202-021-01447-0.
- Tarantola, A. (1986). A strategy for nonlinear elastic inversion of seismic reflection data, Geophysics, 51(10), 1893–1903, https://doi. org/10.1190/1.1442046.
- Virieux, J. & Operto, S. (2009). An overview of fullwaveform inversion in exploration geophysics, Geophysics, 74(6), WCC1–WCC26, https://doi. org/10.1190/1.3238367.
- Triyoso, W., Sinaga, E. I., & Oktariena, M. (2024). Seismic Data Processing and Seismic Inversion in The Ray Parameter Domain: Common Reflection Point (CRP) Stack and Ray Impedance. Scientific Contributions Oil and Gas, 47(2), 129-139. https://doi.org/10.29017/SCOG.47.2.1621.
- Winardhi, S., Sigalingging, A.S., Triyoso, W., Sukmono, S., Dinanto, E., Hendriyana, A., Wardaya, P.D., Septama, E. & Raguwanti, R. (2024). Deep learning-based low-frequency extrapolation: Its implication in 2D full waveform imaging for marine seismic data in the Sadewa Field, Indonesia, First Break, 42(7), 65-72, https://doi.org/10.3997/1365-2397.fb2024059.
- Witte, P.A., Louboutin, M., Kukreja, N., Luporini, F., Lange, M., Gorman, G.J. & Herrmann, F.J. (2019). A large-scale framework for symbolic implementations of seismic inversion algorithms in Julia, Geophysics, 84(3), F57–F71, https://doi.

- org/10.1190/geo2018-0174.1.
- Yu, S., & Ma, J. (2021). Deep learning for geophysics: Current and future trends. Reviews of Geophysics, 59, e2021RG000742. https://doi. org/10.1029/2021RG000742.
- Zhang, Q., Mao, W., Zhou, H., Zhang, H. & Chen, Y. (2018). Hybrid-domain simultaneous-source full waveform inversion without crosstalk noise, Geophysical Journal International, 215(3), 1659–1681, https://doi.org/10.1093/gji/ggy366.